

# Facial-Expression and Gaze-Selective Responses in the Monkey Amygdala

Kari L. Hoffman, Katalin M. Gothard, Michael C. Schmid, and Nikos K. Logothetis

## Supplemental Experimental Procedures

Both monkeys were subordinate to the other monkey(s) in their cages; one was a subadult weighing 7.5 kg, and the other was an adult weighing 11 kg. The monkeys were habituated to peripheral devices, restraint, and scanner sounds during gaze-fixation training in a setup that was designed to simulate the conditions experienced inside the magnet. After the head was restrained, sound-attenuating silicone ear putty was applied and covered with earphones that were secured with sound-attenuating foam. Experimental control was provided through custom-code running on a QNX real-time PC (QNX Software Systems, Canada), which delivered visual stimulation via the Avotec projection system (Avotec, Stuart, FL). A shielded IR-sensitive CCD camera was secured behind the Avotec eyepiece mirror, which, in conjunction with illuminating IR diodes, provided an eye image used for infrared eye-tracking (SensoMotoric Instruments [SMI], Teltow/Berlin, Germany).

For reduction of the occurrence of movement artifacts during acquisition of critical image volumes, monkeys were trained to remain still for the duration of a trial before receiving juice reinforcement. Any changes in jaw position or posture triggered custom-made inductive-coil sensors (designed by A. Oeltermann), and this caused the trial to terminate immediately, without reward.

Training trials began with a period of immobility (i.e., subthreshold sensor activity) and was followed by simultaneous presentation of a tone and the central fixation spot measuring  $0.2^\circ$  visual angle. After a variable fixation duration held within a window of  $0.7^\circ$ – $1.5^\circ$  visual angle, a series of nonface natural images appeared. For monkey 1, the fixation spot disappeared, and gaze within the image boundary was required. For monkey 2, the fixation spot remained, and fixation within  $1^\circ$ – $2^\circ$  visual angle was required.

## Task Design

The six face conditions (threat directed, threat averted, neutral directed, neutral averted, appeasing directed, appeasing averted) were sampled randomly without replacement and the order of the 12 individuals within a block was randomized across, but held constant within, a continuous acquisition period (i.e., “scan”). In this way, any particularly salient or aberrant images would remain in the same position across conditions but would not be fixed over the course of an entire day’s session. As in the training sessions, prior to onset of the first block image, the monkey was required to be still for 2 s and then fixate, while remaining motionless, for 3–6 s (Figure 1C). Stimulus onset was shifted in time with respect to the volume acquisition, in order to better align the maximal BOLD response during the target volume acquisitions (shown in Figure 1C). Each face image was normalized for luminance and contrast (Figure 1A) and placed on a midgray background before undergoing Fourier phase scrambling. Each image subtended a  $10^\circ$  visual angle, was presented for 500 ms, and was followed by 500 ms of a midgray blank square before the next image appeared (Figure 1B). After the 12<sup>th</sup> image, monkeys were required to maintain the same level of fixation for an additional 2 s prior to juice reward, so that the final target volume acquisition could be finished (Figure 1C). Total trial duration was 19–22 s, depending on the speed with which the fixation window was entered and the subsequent alignment to an image-acquisition volume.

## Data Acquisition and Processing

Images were acquired in a vertical, 40-cm-bore 4.7 T magnet (Bruker, Ettlingen, Germany) with a custom-designed transmit and receive saddle coil providing coverage of occipital and temporal lobes (designed by H. Merkle). Structural images included nine-slice IR-RARE images (inversion recovery rapid acquisition relaxation enhanced, [S1]) for facilitating coregistration, as well as 3D MDEF

images ([S2], three-dimensional modified driven equilibrium Fourier transform, [S3]) at 0.5 mm isotropic voxel resolution.

Functional images were acquired from a  $10^\circ$  horizontal slice orientation approximately parallel to the Frankfurt zero plane. For minimization of the strong susceptibility artifacts around the temporal pole and, in particular, along the ventral surface of cortex above the ear canal, several steps were taken. We used eight-segment gradient-echo images with a 17 ms TE and  $40^\circ$  flip angle. A  $12.8 \times 12.8$  cm FOV and a  $128 \times 128$  matrix over nine contiguous 2 mm slices was obtained for a TR of 3 s (i.e., 375 ms for each of eight segments). This yielded four volumes (“target volumes”) for each 12 s stimulus block. Although this greatly reduced the number of volumes used for analysis, movement and susceptibility artifacts were mitigated and thus yielded optimal signal quality in these volumes.

## Analysis

Data preprocessing included concatenation of target volumes, realignment, and spatial and temporal filtering. Target volumes were extracted and concatenated into a pseudocontinuous time course (Figure 1D), provided that all images in that block, and in the respective face or scramble paired blocks were within the motion-detecting limits. From each session, one time course was constructed. Realignment, filtering, and statistical analysis were done with Statistical Parametric Mapping Software (SPM2; Wellcome Department of Imaging Neuroscience, London, UK; <http://www.fil.ion.ucl.ac.uk/spm>), which uses the framework of the general linear model [S4]. Realignment resulted in less than 0.5 mm translation and a  $0.4^\circ$  rotation in any axis for both monkeys. Time courses were high-pass filtered with a cutoff at 128 s and smoothed with an in-plane Gaussian kernel of 1.5 mm full width at half maximum.

The amygdala activation was evaluated further on the basis of the classification of the constituent groups of nuclei. The lateral, basal, and accessory basal nuclei of the amygdala form the basolateral complex of the amygdala (BLA). The BLA receives inputs from extrastriate visual, auditory, and somatosensory cortices [S5–S8] and projects back to the same areas, as well as to other amygdaloid nuclei. The second major cluster of nuclei includes the central nucleus, the bed nucleus of the stria terminalis, and the surrounding areas, collectively called the lateral extended amygdala (LEA). The components of the LEA share inputs and outputs and can be considered a functional unit of the amygdala (e.g., [S9]; reviewed by [S10]). The LEA receives inputs from the basolateral complex and constitutes a major source of autonomic output, via projections to the hypothalamus, basal forebrain, and various brainstem nuclei [S9]. The central nucleus is involved in the initiation of somatic, autonomic, and endocrine responses to arousing stimuli [S11–S13]. Although similar in size and situated adjacent to the central nucleus, the medial nucleus is considered part of an olfactory circuit within the amygdala [S6].

The structural images from each monkey were used for identifying the boundaries of the major amygdaloid nuclei for each monkey, which were then grouped into the following three regions of interest (ROI): the basolateral complex of the amygdala (BLA) containing lateral, basal, and accessory basal nuclei; the lateral extended amygdala (LEA) containing the central nucleus and the bed nucleus of the stria terminalis; and the medial nucleus. Note that we use the term bed nucleus of the stria terminalis to indicate the region of the stria terminalis abutting the central nucleus but do not claim to have resolved the bed nucleus from the coextensive aspect of the stria terminalis. The responses across the face conditions in each ROI are shown relative to activation from the respective scrambled block (Figures 3, inset, and 4, inset). The STS ROI took the 80 voxels surrounding the peak activation in each hemisphere, all of which exceeded significance levels of  $p < 0.00001$  in the Face > Scrambled contrast. The voxel count selected was equal to that of the BLA ROI.

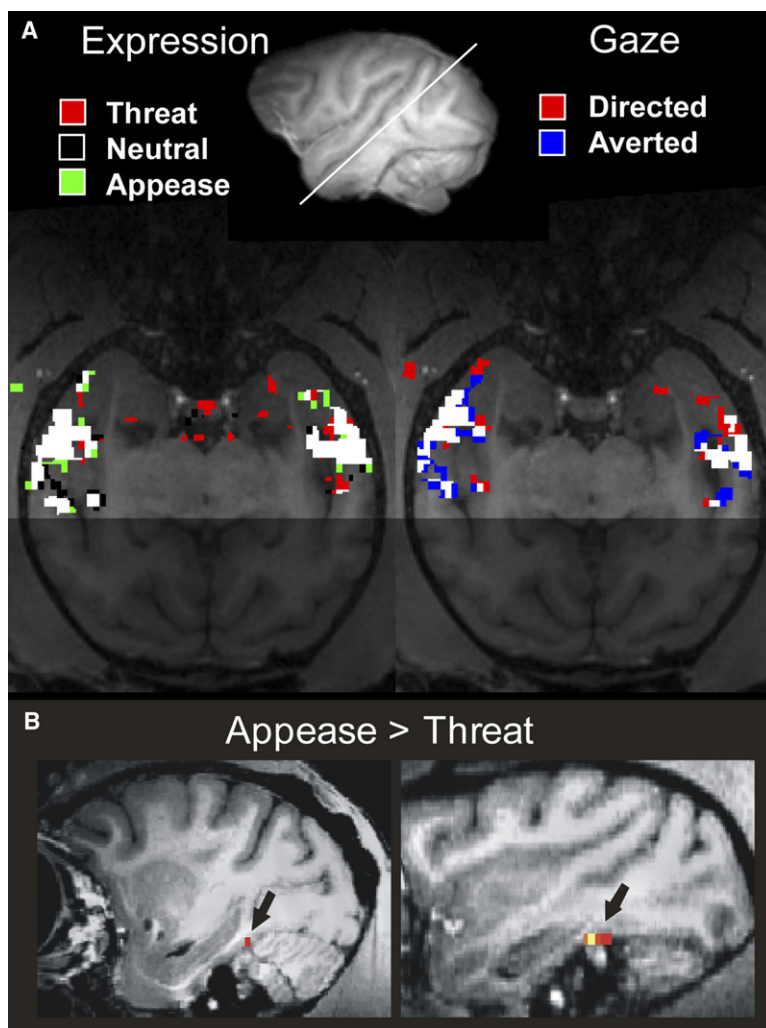


Figure S1. Neocortical Activation for Expressions and Gaze

(A) Overlapping responses to expression (left) and gaze (right) conditions relative to their respective scrambled condition. Images were resliced so that the maximum extent of the superior temporal sulcus was revealed (see slice angle indicated on the rendered brain in the center). White voxels indicate regions of overlapping activation, i.e., voxels that were significant beyond the  $p < 0.01$  threshold for more than one contrast. Areas outside the functional scan regions have been darkened.

(B) Activation for Appease > Threat—the only contrast that produced similar and significant neocortical activation in both monkeys. These areas were also active for the Face > Scrambled contrast; thus, the effect is consistent with differences in activation across conditions, whether these differences are in enhanced activation for appease relative to neutral blocks or in weakened activation for threat relative to neutral blocks. The color map is as shown in Figure 3.

### SCRs

Because of the slow time course of the SCRs, the monkeys were trained to maintain gaze within the image boundary for 3 s and wait 3 s between each image presentation. The order of image presentation was pseudorandom, with images from error trials repeated until the set of all 72 images were viewed. The maximum conductance change from baseline (peak SCR) occurring within a 3 s window starting 1 s after image onset was recorded.

### PPI

Condition-dependent changes of correlations between an ROI and the rest of the brain (psychophysiological interactions or PPIs) were calculated for the two amygdala ROIs in accordance with standard procedures [S14]. This involved a GLM analysis with three regressors, one containing the mean-corrected time course of an ROI, another containing the face or scramble regressor, and the last being the product of the two. Significance for the last regressor would indicate voxels whose activity covaried more with that of the ROI during face blocks than during scrambled blocks. The results are expressed as a statistical map in SPM.

### Facial Expressions in Macaques

Comprehensive descriptions of macaque facial expressions and gestures have sometimes included a “friendly zone” with less polar extremes of the dominance-submission axis [S15] or a three-axis division that distinguishes among the following three “A’s”: aggression, affiliation, and avoidance [S16–S19]. In the latter scheme, both contrasts of dominance versus submission and approach versus avoidance are present: The aggression axis contains expressions

such as the open-mouth threat that is used in this study and that indicates dominance and negative approach; the avoidance axis would include the fear grimace (or bared-teeth grin) of negative avoidance; and the affiliative axis would indicate the lipsmack, inviting friendly approach [S20]. Bridging across species isn’t made easier with this framework, but it does illustrate that multiple models can be used for describing facial expressions. Perhaps in attempting to bridge the species gap we may uncover a common framework that can account for species-specific expressions across a variety of primate species.

### Supplemental References

- S1. Hennig, J., Nauerth, A., and Friedburg, H. (1986). RARE imaging: A fast imaging method for clinical MR. *Magn. Reson. Med.* 3, 823–833.
- S2. Ugurbil, K., Garwood, M., Ellermann, J., Hendrich, K., Hinke, R., Hu, X., Kim, S.G., Menon, R., Merkle, H., and Ogawa, S. (1993). Imaging at high magnetic fields: Initial experiences at 4 T. *Magn. Reson. Q.* 9, 259–277.
- S3. Hochmann, J., and Kellerhals, H. (1980). Proton NMR on deoxyhemoglobin - use of a modified DEFT technique. *J. Magn. Reson.* 38, 23–39.
- S4. Friston, K.J., Holmes, A.P., Worsley, K.J., Poline, J.-P., Frith, C.D., and Frackowiak, R.S.J. (1995). Statistical parametric maps in functional imaging: A general linear approach. *Hum. Brain Mapp.* 2, 189–210.

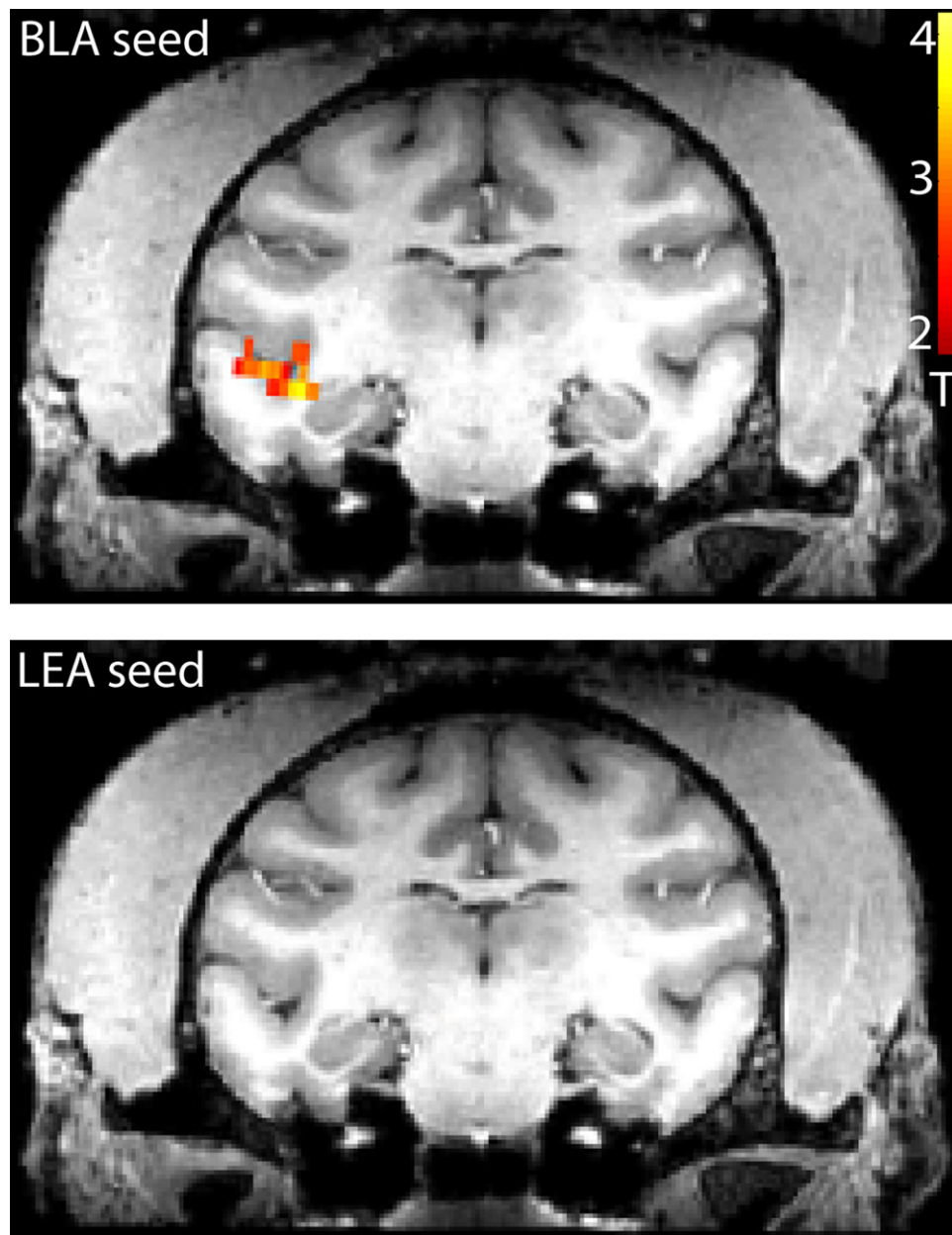


Figure S2. Condition-Specific Coupling between STS and Amygdala Activity

The same coronal section reveals activation in the fundus of posterior STS corresponding to activation in the basolateral complex (top panel) but not the lateral extended amygdala (bottom panel) during presentation of faces but not scrambled images. Functional activation had a threshold of  $p < 0.001$ , uncorrected, no clustering.

- S5. Amaral, D.G., and Price, J.L. (1984). Amygdalo-cortical projections in the monkey (*Macaca fascicularis*). *J. Comp. Neurol.* 230, 465–496.
- S6. Amaral, D.G., Price, J.L., Pitkänen, A., and Carmichael, S.T. (1992). Anatomical organization of the primate amygdaloid complex. In *The Amygdala: Neurobiological Aspects of Emotion, Memory, and Mental Dysfunction*, J.P. Aggleton, ed. (New York: Wiley-Liss), pp. 1–66.
- S7. McDonald, A.J. (1998). Cortical pathways to the mammalian amygdala. *Prog. Neurobiol.* 55, 257–332.
- S8. Aggleton, J.P., Burton, M.J., and Passingham, R.E. (1980). Cortical and subcortical afferents to the amygdala of the rhesus monkey (*Macaca mulatta*). *Brain Res.* 190, 347–368.
- S9. Swanson, L.W., and Petrovich, G.D. (1998). What is the amygdala? *Trends Neurosci.* 21, 323–331.
- S10. Davis, M., and Whalen, P.J. (2001). The amygdala: Vigilance and emotion. *Mol. Psychiatry* 6, 13–34.
- S11. Kaada, B. (1967). Brain mechanisms related to aggressive behavior. *UCLA Forum Med. Sci.* 7, 95–133.
- S12. Moga, M.M., and Gray, T.S. (1985). Evidence for corticotropin-releasing factor, neurotensin, and somatostatin in the neural pathway from the central nucleus of the amygdala to the parabrachial nucleus. *J. Comp. Neurol.* 241, 275–284.
- S13. Kapp, B.S., Frysiner, R.C., Gallagher, M., and Haselton, J.R. (1979). Amygdala central nucleus lesions: Effect on heart rate conditioning in the rabbit. *Physiol. Behav.* 23, 1109–1117.
- S14. Friston, K.J., Buechel, C., Fink, G.R., Morris, J., Rolls, E., and Dolan, R.J. (1997). Psychophysiological and modulatory interactions in neuroimaging. *Neuroimage* 6, 218–229.

Table S1. Brain Regions Showing Significant BOLD Signal Changes across Monkeys

Region	Monkey	Peak (AP/ML)	Number of Voxels*	Max. T Score	p Value $1 \times 10^{-x}$
<b>Faces &gt; Scrambled</b>					
R. STS	1	18, 25	189	19.38	>15
R. STS	2	18, 26	176	10.21	>15
L. STS	1	20, -25	207	14.03	>15
L. STS	2	19, -26	44	11.95	>15
R. Amygdala	1	19, 9	44	4.90	6
R. Amygdala	2	21, 11	9	3.62	3
L. Amygdala	1	19, -12	30	4.24	4
L. Amygdala	2	21, -10	18	3.75	4
<b>Threat &gt; Appease</b>					
R. BLA	1	20, 13	19	3.24	3
R. BLA	2	22, 12	23	3.14	3
L. BLA	1	21, -12	8	2.94	2
L. BLA	2	22, -9	30	2.92	2
<b>Appease &gt; Threat</b>					
R. OTS	1	3, 13	3	3.08	3
R. OTS	2	3, 16	9	4.30	4
<b>Averted &gt; Directed</b>					
R. LEA	1	18, 11	10	4.34	5
R. LEA	2	17, 11	4	3.42	3

\* The number of active voxels is based on a statistical threshold of  $p < 0.001$  for Faces > Scrambled and a cutoff of  $p < 0.01$  for all other contrasts.

Table S2. Two-Way ANOVA Results for Expression  $\times$  Gaze

Source	Condition	F Score	p Value
<b>BLA</b>			
	<u>Expression</u>	<u>10.35</u>	<u>0.000</u>
	Gaze	0.46	0.498
	Interaction	0.56	0.573
<b>MED</b>			
	Expression	1.35	0.262
	Gaze	0.46	0.498
	Interaction	0.31	0.731
<b>LEA</b>			
	Expression	0.80	0.452
	<u>Gaze</u>	<u>6.84</u>	<u>0.007</u>
	Interaction	0.14	0.871
<b>STS</b>			
	Expression	0.94	0.391
	Gaze	0.75	0.386
	Interaction	0.94	0.394
<b>SCR</b>			
	Expression	0.01	0.986
	<u>Gaze</u>	<u>8.23</u>	<u>0.002</u>
	Interaction	1.06	0.347

The underlined data indicate the results that were statistically significant.

- S15. Maxim, P.E. (1982). Contexts and messages in macaque social communication. *Am. J. Primatol.* 2, 63–85.
- S16. Deputte, B.L. (1983). Ontogenic development of dyadic social relationships - assessing individual roles. *Am. J. Primatol.* 4, 309–318.
- S17. Deputte, B. (2000). Primate socialization revisited: Theoretical and practical issues in social ontogeny. *Advances in the Study of Behavior* 29, 99–157.
- S18. Partan, S.R. (2002). Single and multichannel signal composition: Facial expressions and vocalizations of rhesus macaques (*Macaca mulatta*). *Behaviour* 139, 993–1027.
- S19. Mason, W.A. (1985). Experiential influences on the development of expressive behaviors in rhesus monkeys. In *The development of expressive behavior: Biology-environment interactions*, G. Zivin, ed. (New York: Academic Press), pp. 117–152.
- S20. Maestripieri, D., and Wallen, K. (1997). Affiliative and submissive communication in rhesus macaques. *Primates* 38, 127–138.